Received ; | Revised ; | Accepted

DOI: xxx/xxxx

RESEARCH ARTICLE

An iterative method for optimal control of bilateral free boundaries problem

Youness El Yazidi* | Abdellatif Ellabib

[1]Laboratory of Applied Mathematics and Computer Science, Faculty of Science and Technology, Cadi Ayyad University, Marrakesh, Morocco

Correspondence
*Corresponding Y. EL Yazidi Email: youness.elyazidi@edu.uca.ac.ma

Summary

The aim of this paper is to construct a numerical scheme for solving a class of bilateral free boundaries problem. First, using a shape functional and some regularization terms, an optimal control problem is formulated, in addition, we prove its solution existence's. The first optimality conditions and the shape gradient are computed. the proposed numerical scheme is a genetic algorithm guided conjugate gradient combined with the finite element method, at each mesh regeneration, we perform a mesh refinement in order to avoid any domain singularities. Some numerical examples are shown to demonstrate the validity of the theoretical results, and to prove the robustness of the proposed scheme.

KEYWORDS:
Adaptive mesh-refinement techniques, Conjugate Gradient method, Genetic Algorithm, Inverse problem, Regularization, Shape optimization

1 | INTRODUCTION

Let Ω be an open set in $\mathbb{R}^2$ whose boundary parts Γ_1 and Γ_2 are unknown (figure 1). For a given pair of data $(g_1, g_2) \in H^{1/2}(\partial\Omega) \times H^{-1/2}(\partial\Omega)$, let consider following class of elliptic boundary value problem:

$$\begin{cases} -\nabla(A\nabla u) = f & \text{in} \quad \Omega \\ u = g_1 & \text{on } \partial\Omega, \\ A\nabla_\nu u = g_2 & \text{on } \partial\Omega \end{cases} \tag{1}$$

with f and A are known functions. And ν is the normal unit outer vector.

The aim of this paper is to perform the mathematical analysis and to construct a numerical scheme for the inverse identification problem of the free boundaries Γ_1 and Γ_2. This kind of inverse problem can model for example, the identification of depletion region in semiconductor, the multi-phase Stefan problem, cavities identification[1,2,3].

Let first assume that the free boundaries are parametrized as follow

$$\Gamma_1(\varphi) = \{(\varphi(y), y) : \ L_1^0 \le \varphi(y) \le L_1^1 \text{ and } y \in [a, b]\}$$
$$\Gamma_2(\psi) = \{(\psi(y), y) : \ L_2^0 \le \psi(y) \le L_2^1 \text{ and } y \in [a, b]\},$$

and an admissible domain Ω by

$$\Omega(\varphi, \psi) = \{(x, y) : \ \varphi(y) < x < \psi(y) \text{ and } y \in [a, b]\} \subseteq D$$

[0]**Abbreviations:** CG, conjugate gradient; GAs, Genetic algorithms

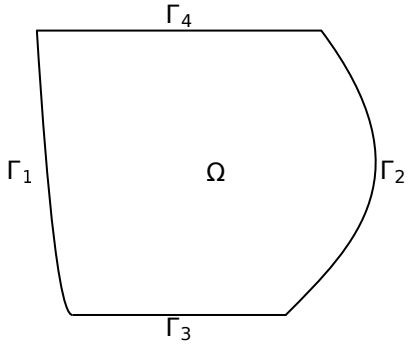

FIGURE 1 Geometry of Ω.

with D is a fixed open set in $\mathbb{R}^2$. Then set of the admissible shapes Θ_{ad} is given by:

$$\Theta_{ad} = \left\{ \Omega(\varphi,\psi)/(\varphi,\psi) \in (C([a,b]))^2,\ \varphi \text{ and } \psi \text{ are Lipschitz functions} \right\}.$$

We note that Γ_1 and Γ_2 must not intersect, thus we assume that $L_1^1 < L_2^0$. The space Θ_{ad} is endowed with the Hausdorff topology.

The system (1) is overdetermined, this is means that for any admissible domain $\Omega \in \Theta_{ad}$ and a given pair of data (g_1, g_2) in $H^{1/2}(\partial\Omega) \times H^{-1/2}(\partial\Omega)$, it may not exist any optimal solution $u \in H^1(\Omega)$ to the system (1).

Our aim is to identify the configuration of the free boundaries Γ_1 and Γ_2 (e.g. the configuration of Ω) using the pair of Dirichlet and Neumann data (g_1^ρ, g_2^ρ) of the exact data (g_1, g_2) satisfying

$$\|g_1^\rho - g_1\|_{H^{1/2}(\partial\Omega)} + \|g_2^\rho - g_2\|_{H^{-1/2}(\partial\Omega)} \leq \rho.$$

with ρ stand for the noise level.

Throughout the rest of the paper we need the following assumptions

A1: $f \in L^2(D)$ is a continuous.

A2: $A \in L^\infty(D)$, continuous function, that satisfy there exist $a_m, a_M > 0$ such that

$$(A(x)\xi,\xi) \geq a_m|\xi|^2 \text{ and } |A(x)\xi| \leq a_M|\xi| \quad \forall \xi \text{ a.e. in } D$$

Now, the overdetermined system (1) will be split into two well posed problem, for that let consider the following spaces:

$$\mathrm{U}_d^1 = \left\{u \in H^1(\Omega),\ \ u = g_1^\rho \text{ on } \Sigma_1\right\}, \quad \mathrm{U}_0^1 = \left\{u \in H^1(\Omega),\ \ u = 0 \text{ on } \Sigma_1\right\}$$
$$\mathrm{U}_d^2 = \left\{u \in H^1(\Omega),\ \ u = g_1^\rho \text{ on } \Sigma_2\right\}, \quad \mathrm{U}_0^2 = \left\{u \in H^1(\Omega),\ \ u = 0 \text{ on } \Sigma_2\right\}$$

with $\Sigma_1 = \Gamma_1 \cup \Gamma_2$ and $\Sigma_2 = \Gamma_3 \cup \Gamma_4$, $H^1(\Omega)$ is the usual Sobolev space.

The first state problem reads

$$-\nabla(A\nabla u) = f \text{ in } \Omega, \quad u = g_1 \text{ on } \Sigma_1 \quad \text{and} \quad A\nabla_\nu u = g_2^\rho \text{ on } \Sigma_2, \tag{2}$$

we associate it to the variational equation, for any $v \in \mathrm{U}_0$ we write

$$\mathcal{E}_1(\Omega,u) = \int_\Omega A\nabla u\nabla v dx - \int_\Omega f v dx - \int_{\Sigma_2} g_2^\rho v d\sigma \tag{3}$$

We denote by $u_1 \in \mathrm{U}_d^1$ the unique solution of (3), which is guaranteed by Lax-Milgram theorem. The second state equation is defined by

$$-\nabla(A\nabla u) = f \text{ in } \Omega, \quad u = g_1^\rho \text{ on } \Sigma_2 \quad \text{and} \quad A\nabla_\nu u = g_2^\rho \text{ on } \Sigma_1, \tag{4}$$

associated to the variational form, for any $v \in H^1(\Omega)$ we have

$$\mathcal{E}_2(\Omega,u) = \int_\Omega A\nabla u\nabla v dx - \int_\Omega f v dx - \int_{\Sigma_1} g_2^\rho v d\sigma \tag{5}$$

similarly, the Lax-Milgram theorem ensure the existence of a unique solution of (5) in U_d^2 denoted u_2. The next step, we introduce the Kohn-Volgelius cost functional:

$$J(\Omega, u_1, u_2) = \frac{1}{2} \int_{\Omega} A \left| \nabla(u_1 - u_2) \right|^2 dx \tag{6}$$

Let define the following spaces

$$\mathcal{U}_1 = \left\{ u \in \mathrm{U}_d^1 \ : \ \mathcal{E}_1(\Omega, u) = 0 \right\} \text{ and } \mathcal{U}_2 = \left\{ u \in \mathrm{U}_d^2 \ : \ \mathcal{E}_2(\Omega, u) = 0 \right\},$$

the shape optimization problem is summarized as follows:

$$\min_{(\Omega, u_1, u_2) \in \mathcal{F}} J(\Omega, u_1, u_2) \tag{7}$$

where $\mathcal{F} = \Theta_{ad} \times \mathcal{U}_1 \times \mathcal{U}_2$. With the Hausdorff topology we can not prove the existence of an optimal solution of problem (7), especially for the Dirichlet problem[4] to overcome this issue, a regularization term[4] is added, we are interested then in the following optimal control problem

$$\min_{(\Omega, u_1, u_2) \in \mathcal{F}} J(\Omega, u_1, u_2) + \varrho_1 \mathcal{P}(\Omega) \tag{8}$$

$\varrho_1 > 0$ is a regularization coefficient, $\mathcal{P}$ is the perimeter of Ω. Now with the results of Sokolowski and Zolesio[4], problem (8) admit at least an optimal solution. Our contribution aim to add another accurate control term, for that we consider $\mathcal{O}$ a fixed domain of Θ_{ad}, we define $\mathcal{R}(\Omega) = \mathrm{meas}(\Omega \Delta \mathcal{O})$, let consider then the new optimal control problem

$$\min_{(\Omega, u_1, u_2) \in \mathcal{F}} \mathcal{J}(\Omega, u_1, u_2) := J(\Omega, u_1, u_2) + \varrho_1 \mathcal{P}(\Omega) + \varrho_2 \mathcal{R}(\Omega) \tag{9}$$

with $\varrho_2 > 0$ is a penalty coefficient, . The latter term in $\mathcal{J}$ means that we are looking for the control domain Ω that covers $\mathcal{O}$.

There are some works studying the optimal control problems derived of shape optimization problems. In the work[5], the authors studied an optimal control of bilateral obstacle problem using variational inequalities. Hinze and Ziegenbalg in[6] studied an optimal control problem of the evolution of a free boundary in the two phase Stefan problem, they also proposed an numerical scheme based on the finite difference method on a moving grid.

Several iterative schemes were proposed to solve similar identification problem, in[2] the authors proposed a conjugate gradient method and boundary element for the identification of two interfaces in a region of three sub domains. Mozaffari et al.[3] studied the identification problem of two interfaces using the boundary element method combined with the imperialist competitive algorithm guided the conjugate gradient/Simplex method.

The iterative scheme proposed here, to solve the optimal control problem (9), is a combined genetic algorithm guided the conjugate gradient method with the finite element. The motivation behind the genetic algorithms comes for picking the best initial guess for the gradient method, to avoid the manually choice that may affect the convergence of the gradient method. There are some papers used the genetic algorithms (GAs) in the approximation of free boundary problems. In the work[7], the authors combined GAs with the conjugate gradient and the boundary element method for the identification of cavities. In[8] the authors used the genetic algorithm with the finite element to estimate the configuration of depletion layer in semiconductor.

One frequent difficulty accuracies in the numerical approximation is dealing with domains with singularities, for example, domains with corners or intern boundaries. To over come this, we propose to use adaptive refinement mesh techniques, to refine the triangulation near to the singularities, An a posteriori error estimate is need for performing a mesh refinement. In[9] the mesh refinement was proposed to improve the quality of FEM approximation in shape optimization problems, they considered the norm of the Lagrange augmented functional variation with respect to the boundary variation as their a posteriori error estimate. In[10] adaptive mesh refinement was used in moving interfaces approximation basing on level set method.

In what follows, we prove the unique existence of solution of the optimal control problem (9). In section 3 we establish the first optimality condition and we compute the shape gradient. The convergence of the discrete optimal design problem is proved in section 4. In the fifth section, we describe the manipulation of the adaptive mesh refinement. In section 6 we give all the step for the proposed iterative scheme. In the last section, we perform some numerical examples to illustrate the validity of the theoretical results and to prove the efficiency of the proposed scheme.

2 | EXISTENCE OF AN OPTIMAL SHAPE

As we mentioned in the introduction, the assumptions **A1-A2** with the Lax-Milgram theorem ensure the solution existence of problems (3) and (5), in addition we have the following estimates

Lemma 1. For any $\Omega \in \Theta_{ad}$, there exist $M_1, M_2 > 0$ such that

$$|u_1|_{1,\Omega} \leq M_1 \quad \text{and} \quad |u_2|_{1,\Omega} \leq M_2 \tag{10}$$

The proof of this lemma is classic. Now we prove the following result

Lemma 2. The space of feasible solutions $\mathcal{F}$ is compact.

Proof. Let $(\Omega_n, u_{1,n}, u_{2,n})$ be a sequence of $\mathcal{F}$, we shall prove the existence of a subsequence of $(\Omega_n, u_{1,n}, u_{2,n})$ that converges in $\mathcal{F}$.

First we have $\Omega_n = \Omega(\varphi_n, \psi_n)$, using Ascoli-Arzéla theorem we ensure that (φ_n, ψ_n) that converges uniformly as a subsequence to an element (φ, ψ). It is easy to deduce that $\Omega = \Omega(\varphi, \psi)$ lives in Θ_{ad}.

Since $u_{1,n}$ and $u_{2,n}$ are bounded, we can use the Rellich theorem to show the existence of u_1 and u_2 such that $u_{1,n}$ converges weakly to u_1 in $H^1(D)$ resp. $u_{2,n}$ converges weakly to u_2 in $H^1(D)$. We ought to prove that $u_1 \in \mathcal{U}_1$ and $u_2 \in \mathcal{U}_2$. We first show that u_1 satisfy (3), for that we will only prove the convergence

$$\lim_{n\to\infty} \int_{\Omega_n} A\nabla u_{1,n}\nabla v dx = \int_{\Omega} A\nabla u_1 \nabla v dx \tag{11}$$

we have

$$\int_{\Omega_n} A\nabla u_{1,n}\nabla v dx - \int_{\Omega} A\nabla u_1 \nabla v dx = \int_{1} (\chi_{\Omega_n} - \chi_{\Omega}) A\nabla u_{1,n}\nabla v dx + \int_{\Omega} A\nabla(u_{1,n} - u_1)\nabla v dx$$

Since Ω_n converge to Ω in Hausdorff topology then χ_{Ω_n} converges to χ_{Ω} in $L^\infty(D)$ weak star, also we have that $\nabla u_{1,n}$ converges weakly to ∇u_1, thus proves that (11) is hold. At this end we have proved that u_1 satisfy (3), to conclude this proof we have to show that $u_1 \in \mathrm{U}_d^1$

The fact that $\Gamma_{1,n} \cup \Gamma_{2,n}$ is not fixed, we can not apply the trace operator directly to deduce that $u_1 = g_3$ on $\Gamma_1 \cup \Gamma_2$. It can be overcome by proving that

$$\lim_{n\to\infty} \int_{\Gamma_{1,n}\cup\Gamma_{2,n}} |u_{1,n}|^2 dx = \int_{\Gamma_1\cup\Gamma_2} |u_1|^2 dx \tag{12}$$

We have then

$$\int_{\Gamma_{1,n}\cup\Gamma_{2,n}} |u_{1,n}|^2 dx - \int_{\Gamma_1\cup\Gamma_2} |u_1|^2 dx = \int_{1} (\chi_{\Gamma_{1,n}\cup\Gamma_{2,n}} - \chi_{\Gamma_1\cup\Gamma_2}) |u_{1,n}|^2 dx + \int_{\Gamma_1\cup\Gamma_2} \left[|u_{1,n}|^2 - |u_1|^2\right] dx$$

with the above convergence we infer (12). Finally $u_1 \in \mathcal{U}_1$, similarly we can show that $u_2 \in \mathcal{U}_2$. At this end we have proved the existence of a subsequence of $(\Omega_n, u_{1,n}, u_{2,n})$ that converges in $\mathcal{F}$. □

Lemma 3. The functional $\mathcal{J}$ is semi lower continuous on $\mathcal{F}$.

Proof. Let $(\Omega_n, u_{1,n}, u_{2,n})$ be a sequence that converge to (Ω, u_1, u_2) in $\mathcal{F}$, we need to show that

$$\mathcal{J}(\Omega, u_1, u_2) \leq \liminf_{n\to+\infty} \mathcal{J}(\Omega_n, u_{1,n}, u_{2,n})$$

For that we will show that $(u_{1,n})$ and $(u_{2,n})$ converge strongly. Since the embedding of $H^1(D)$ is compact in $L^2(D)$, the sequence $(u_{1,n})$ converges strongly to u_1 in $L^2(D)$. We have also that

$$\begin{aligned}\int_{D} |\nabla(u_{1,n} - u_1)|^2 dx \leq & \frac{1}{a_m} \int_{1} A|\nabla(u_{1,n} - u_1)|^2 dx \\ \leq & \int_{\Omega} f(u_{1,n} - u_1) dx + \int_{\Sigma_2} g_2^{\rho}(u_{1,n} - u_1) d\sigma\end{aligned}$$

The right hand side of the latter inequality vanishes, thereafter $(\nabla u_{1,n})$ converges strongly to ∇u in $\left[L^2(D)\right]^2$, hence $(u_{1,n})$ converges strongly to u_1 in $H^1(D)$. Similarly we obtain $(u_{2,n})$ converges strongly to u_2 in $H^1(D)$

Now it is easy to deduce that

$$\lim_{n\to+\infty} J(\Omega_n, u_{1,n}, u_{2,n}) = J(\Omega, u_1, u_2)$$

Since Ω_n converges to Ω then we have (φ_n, ψ_n) converges uniformly to (φ, ψ), which implies that $\mathcal{P}(\Omega) \leq \liminf_{n\to+\infty} \mathcal{P}(\Omega_n)$, and $\mathcal{R}(\Omega) \leq \liminf_{n\to+\infty} \mathcal{R}(\Omega_n)$, therefore

$$\mathcal{J}(\Omega, u_1, u_2) \leq \liminf_{n\to+\infty} \mathcal{J}(\Omega_n, u_{1,n}, u_{2,n})$$

□

Theorem 1. The optimal control problem (9) has at least a solution in $\mathcal{F}$

Using lemmas 2 and 3 we can easily prove this theorem.

3 | FIRST OPTIMALITY CONDITION

In this section we compute the shape derivative, before that, we recall some practical techniques in shape calculus. Let introduce the fictitious time t, we define the next perturbation operator

$$\mathrm{T}_t = \mathrm{id} + tV$$

whit V is a vector field belongs to the set

$$\Lambda = \left\{ V \in C^{1,1}\left(\overline{\Omega}, \mathbb{R}^2\right) : V|_{\partial\Omega\setminus(\Gamma_1\cup\Gamma_2)} = 0 \right\}$$

We note that T_t is Lipschitz bijective operator, moreover its inverse is Lipschitz continuous[4]. This brings us to define the family of perturbed domains and boundaries

$$\Omega_t = \mathrm{T}_t(\Omega) \quad \text{and} \quad \Gamma_t = \mathrm{T}_t(\Gamma)$$

The state solution on Ω_t is denoted $u_{i,t} \in \mathrm{U}_d$, for $i = 1, 2$.

Definition 1. The material derivative of the state u_i is denoted $u_i' \in \mathrm{U}_d^i$, it is defined by the limit

$$u_i' = \lim_{t\to 0} \frac{u_i^t - u_i}{t}$$

with $u_i^t = u_{i,t} \circ T_t$, for $i = 1, 2$.

Definition 2. Let L be a shape functional, $\Omega \in \Theta_{ad}$ and $V \in \Lambda$, we call the Eulerian derivative of L at Ω in the direction V the quantity

$$\mathrm{d}L(\Omega)V = \lim_{t\to 0} \frac{L\left(\Omega_t\right) - L(\Omega)}{t}$$

if exists. Moreover L is said shape differentiable if $\mathrm{d}L(\Omega)V$ exists $\forall\, V \in \Lambda$.

Remark 1. The material derivative u_i' satisfy the variational equation

$$\int_\Omega \nabla u_i' \nabla w \mathrm{d}x = \int_\Omega \nabla u_i^\top \left[DV + DV^\top - \mathrm{div}(V)I\right] \nabla w + \mathrm{div}(fV) w \mathrm{d}x \tag{13}$$

for $i = 1, 2$.

Now we recall the shape derivative[11,4] for functions depending on Ω or Γ, let consider the shape functionals

$$L_1(\Omega_t) = \int_{\Omega_t} u(t, x) dx \quad \text{and} \quad L_2(\Omega_t) = \int_{\Gamma_t} u(t, s) ds$$

Lemma 4. Let $u \in W^{1,1}(D)$ and $V \in \Lambda$, then the shape functional L_1 is shape differentiable, and we have

$$\mathrm{d}L(\Omega)[V] = \int_\Omega u'(0, x) \mathrm{d}x + \int_{\partial\Omega} u(0, s) V \cdot \nu \mathrm{d}s$$

Similarly, for $u \in W^{2,1}(D)$ and $V \in \Lambda$, then the shape functional L_2 is shape differentiable, and we have

$$\mathrm{d}L(\Omega)[V] = \int_\Gamma u'(0, s) \mathrm{d}s + \int_\Gamma \left(\nabla_\nu u(0, s) + u(0, s)\kappa\right) V \cdot \nu \mathrm{d}s$$

where κ is the mean curvature of the boundary Γ.

Now, we define the Eulerian derivative u_1' and u_2' of the states u_1 and u_2 as solution of the next two problems

$$\begin{cases} -\operatorname{div}(A\nabla u_1') &= 0 & \text{in } \Omega, \\ u_1' &= \nabla_\nu(g_1^\rho - u_1)V\cdot\nu & \text{on } \Sigma_1 \\ A\nabla_\nu u_1' &= 0 & \text{on } \Sigma_2, \end{cases} \tag{14}$$

$$\begin{cases} -\operatorname{div}(A\nabla u_2') &= 0 & \text{in } \Omega, \\ u_2' &= 0 & \text{on } \Sigma_2, \\ A\nabla_\nu u_2' &= G(u_2, V) & \text{on } \Sigma_1 \end{cases} \tag{15}$$

with

$$G(u_2, V) = \operatorname{div}_\Gamma\left(\langle V,\nu\rangle\nabla_\Gamma u_2\right) + \langle V,\nu\rangle\left(\frac{\partial g_2^\rho}{\partial\nu} + \kappa g_2^\rho + f\right)$$

Now we prove the following result

Lemma 5. The functional $\mathcal{J}$ is shape differentiable, its Eulerian derivative in direction $V\in\Lambda$ is given by:

$$d\mathcal{J}(\Omega)[V] = \int_{\Gamma_1\cup\Gamma_2}\left[A\nabla_\nu(u_1-u_2-\lambda_1)\nabla_\nu(g_1^\rho-u_1) - \nabla_\Gamma u\nabla_\nu\lambda_2 + \left(\frac{\partial g_2^\rho}{\partial\nu}+\kappa g_2^\rho + f\right)\lambda_2 + \kappa + 1\right]\langle V,\nu\rangle ds \tag{16}$$

Proof. First, let define the Lagrangian functional $\mathcal{L}$ associated to the cost functional J defined in (6), for an element $(\Omega, u_1, u_2, v_1, v_2)$ in $\theta_{ad}\times \mathrm{U}_d^1\times\mathrm{U}_d^2\times\mathrm{U}_0^1\times\mathrm{U}_0^2$ we define the Lagrangian functional by

$$\mathcal{L}(\Omega, u_1, u_2, v_1, v_2) = \mathcal{J}(\Omega, u_1, u_2) + \mathcal{E}_1(\Omega,\lambda_1) + \mathcal{E}_2(\Omega,\lambda_2) \tag{17}$$

The adjoint solution λ_1 and λ_2 can be computed using the optimality conditions on u_1 and u_2,

$$\frac{\partial\mathcal{L}}{\partial u_1}\cdot\lambda_1 = 0 \quad\text{and}\quad \frac{\partial\mathcal{L}}{\partial u_2}\cdot\lambda_2 = 0$$

which implies the following adjoint problems

$$\begin{cases} -\nabla(A\nabla\lambda_1) &= \nabla(A\nabla(u_1-u_2)) & \text{in } \Omega, \\ \lambda_1 &= 0 & \text{on } \Sigma_1 \\ A\nabla_\nu\lambda_1 &= -A\nabla_\nu(u_1-u_2) & \text{on } \Sigma_2, \end{cases} \tag{18}$$

$$\begin{cases} -\nabla(A\nabla\lambda_2) &= \nabla(A\nabla(u_2-u_1)) & \text{in } \Omega, \\ \lambda_2 &= 0 & \text{on } \Sigma_2 \\ A\nabla_\nu\lambda_2 &= -A\nabla_\nu(u_2-u_1) & \text{on } \Sigma_1, \end{cases} \tag{19}$$

To prove (16), we differentiate each term in $\mathcal{J}$ separately, we start by the functional J, using lemma 4 we have

$$\begin{aligned} dJ(\Omega)[V] &= \int_\Omega A\nabla(u_1'-u_2')\nabla(u_1-u_2)dx + \frac{1}{2}\int_\Gamma|\nabla(u_1-u_2)|^2V\cdot\nu ds \\ &= \int_\Omega A\nabla u_1'\nabla(u_1-u_2)dx - \int_\Omega A\nabla u_2'\nabla(u_1-u_2)dx + \frac{1}{2}\int_{\Sigma_1}|\nabla(u_1-u_2)|^2V\cdot\nu ds \end{aligned}$$

we write

$$\begin{aligned} \int_\Omega A\nabla u_1'\nabla(u_1-u_2)dx &= -\int_\Omega\nabla(A\nabla(u_1-u_2))u_1'dx + \int_{\partial\Omega}A\nabla_\nu(u_1-u_2)u_1'ds \\ &= \int_\Omega\nabla(A\nabla\lambda_1)u_1'dx + \int_{\partial\Omega}A\nabla_\nu(u_1-u_2)u_1'ds \end{aligned}$$

from another hand

$$\begin{aligned} \int_\Omega\nabla(A\nabla\lambda_1)u_1'dx &= -\int_\Omega A\nabla\lambda_1\nabla u_1'dx + \int_{\partial\Omega}A\nabla_\nu\lambda_1u_1'dx \\ &= \int_\Omega\nabla(A\nabla u_1')\lambda_1dx - \int_{\partial\Omega}A\nabla_\nu u_1'\lambda_1dx + \int_{\partial\Omega}A\nabla_\nu\lambda_1u_1'dx \end{aligned}$$

thus

$$\int_{\Omega} A\nabla u_1'\nabla(u_1-u_2)dx = -\int_{\partial\Omega} A\nabla_\nu u_1'\lambda_1 dx + \int_{\partial\Omega} A\nabla_\nu\lambda_1 u_1' dx + \int_{\partial\Omega} A\nabla_\nu(u_1-u_2)u_1' ds$$

Using the informations on the state derivative u_1' and the adjoint solution λ_1 we infer that

$$\int_{\Omega} A\nabla u_1'\nabla(u_1-u_2)dx = \int_{\Sigma_1} A\nabla_\nu(u_1-u_2-\lambda_1)\nabla_\nu(g_1^\rho-u_1)V\cdot\nu ds \tag{20}$$

Similarly we obtain that

$$\int_{\Omega} A\nabla u_2'\nabla(u_1-u_2)dx = \int_{\Sigma_1} G(u_2,V)\lambda_2 ds$$

thereafter

$$\int_{\Omega} A\nabla u_2'\nabla(u_1-u_2)dx = \int_{\Sigma_1}\left[\left(\frac{\partial g_2^\rho}{\partial\nu}+\kappa g_2^\rho+f\right)\lambda_2-\nabla_{\Sigma_1}u_2\nabla\lambda_2\right]\langle V,\nu\rangle ds \tag{21}$$

Now we treat the regularization term $\mathcal{P}(\Omega)$, first we note that

$$\mathcal{P}(\Omega) = \int_{\partial\Omega_t} ds_t,$$

with lemma 4 we deduce

$$d\mathcal{P}(\Omega)[V] = \int_{\Gamma_1\cup\Gamma_2}\kappa\langle V,\nu\rangle ds. \tag{22}$$

It remain the latter term in $\mathcal{J}$. We have $\mathcal{R}(\Omega)=\Omega\Delta\mathcal{O}=(\Omega\setminus\mathcal{O})\cup(\mathcal{O}\setminus\Omega)$, it is easy to remark that the moving part of $\Omega\Delta\mathcal{O}$ is $\Gamma_1\cup\Gamma_2$ then with lemma 4 we infer that

$$d\mathcal{R}(\Omega)[V] = \int_{\Sigma_1}\langle V,\nu\rangle ds \tag{23}$$

Gathering the equalities 20, 21, 22 and 23 we conclude this proof. □

4 | CONVERGENCE OF THE DISCRETE OPTIMAL CONTROL PROBLEM

Let consider $\Omega\in\Theta_{ad}$ and $h>0$ a discretization fineness step, $\mathcal{T}_h$ a family of triangulation of Ω that satisfy the assumptions

A3: For any $T_1,T_2\in\mathcal{T}_h$, T_1 and T_2 share at most a common edge or vertex.

A4: All the triangles in $\mathcal{T}_h$ are regular.

We define the sets

$$\mathtt{E}_h=\bigcup_{T\in\mathcal{T}_h}\mathtt{E}(T)\quad\text{and}\quad\mathtt{N}_h=\bigcup_{T\in\mathcal{T}_h}\mathtt{N}(T)$$

with $\mathtt{E}(T)$ and $\mathtt{N}(T)$ are respectively the edges and the vertices of a triangle T from $\mathcal{T}_h$. Consider Now the discrete space

$$\mathtt{P}_h=\left\{v_h\in C(\overline{\Omega}):\quad v_{h/_T}\in\mathbb{P}_1(T),\quad\forall T\in\mathcal{T}_h\right\}$$

with $\mathbb{P}_1$ is the space of polynomial whose degree does not exceed 1 on $\mathbb{R}^2$. Now we consider the discrete spaces

$$\mathtt{U}_{d,h}^1=\mathtt{U}_d^1\cap\mathtt{P}_h,\quad\mathtt{U}_{0,h}^1=\mathtt{U}_0^1\cap\mathtt{P}_h,\quad\mathtt{U}_{d,h}^2=\mathtt{U}_d^2\cap\mathtt{P}_h\quad\text{and}\quad\mathtt{U}_{0,h}^2=\mathtt{U}_0^2\cap\mathtt{P}_h$$

We have the discrete state solutions satisfy the following, for all $(v_{1,h},v_{2,h})$ in $\mathtt{U}_{0,h}^1\times\mathtt{U}_{0,h}^2$

$$\mathcal{E}_1(\Omega_h,u_{1,h}) = \int_{\Omega_h} A\nabla u_{1,h}\nabla v_{1,h}dx - \int_{\Omega_h} f_h v_{1,h}dx - \int_{\Sigma_{2,h}} g_{2,h}v_{1,h}d\sigma \tag{24}$$

$$\mathcal{E}_2(\Omega_h,u_{2,h}) = \int_{\Omega_h} A\nabla u_{2,h}\nabla v_{2,h}dx - \int_{\Omega_h} f_h v_{2,h}dx - \int_{\Sigma_{1,h}} g_{2,h}v_{2,h}d\sigma \tag{25}$$

Now the discrete control problem reads

$$\min_{(\Omega_h,u_{1,h},u_{2,h})\in\mathcal{F}_h} \mathcal{J}(\Omega_h,u_{1,h},u_{2,h}) := J(\Omega_h,u_{1,h},u_{2,h}) + \varepsilon\mathcal{P}(\Omega_h) + \varrho\mathcal{R}(\Omega_h) \tag{26}$$

with $\mathcal{F}_h = \Theta_{ad,h} \times \mathcal{U}_{1,h} \times \mathcal{U}_{2,h}$,

Lemma 6. Let consider $\Omega \in \theta_{ad}$, u_1 and u_2 the continuous solution of (3) and (5) on Ω, $u_{1,h}$ and $u_{2,h}$ the discrete solution of (24) and (25) on Ω_h. From [12] there exist a constant $C > 0$ such that:

$$\|u_1 - u_{i,h}\|_{\infty,D} \leq Ch|\log h| \quad \text{for} \quad i = 1, 2. \tag{27}$$

Now, let define the following distance

$$\mathrm{d}\left(\Omega,\Omega_h\right) = \inf\left\{r : x \in \Omega, \text{ such that } B(x,r) \subset \left(\Omega\Delta\Omega_h\right)\right\} \tag{28}$$

Theorem 2. Consider (Ω, u_1, u_2) solution of (9), we assume that $(u_1, u_2) \in \left[H^2(\Omega) \cap W^{1,\infty}(\Omega)\right]^2$, there exists a pair $(\Omega_h, u_{1,h}, u_{2,h})$ minimizer of (26), such that

$$\exists C > 0, \quad d\left(\Omega,\Omega_h\right) \leq Ch|\log h| \tag{29}$$

Proof. For h sufficiently small, consider $\mathcal{T}_h$ a triangulation on Ω, the results of Bartles [13] yield to the existence of $(\Omega_h, u_{1,h}, u_{2,h})$ solution of the discrete optimal problem (26), such that $u_{1,h}$ and $u_{2,h}$ satisfy (27). Still to show the estimate (29).

We have for all $I \subset \partial\Omega$, there exists a function $b_I \in C^2(I)$ satisfying

$$\partial\Omega = \bigcup_{I\in\mathcal{T}_h, I\subset\partial\Omega} \left\{x + b_I(x)n_I : x \in I\right\}$$

with n_I is the unit outer normal vector on I, b_I is local parametrization of $\partial\Omega$. If $x \in \mathbb{N}_h \cap S$ then $b_I(x) = 0$, with $\mathbb{N}_h$ is the set of all nodes of $\mathcal{T}_h$, that implies $\left|b_I(x)\right| \leq Ch|\log h|$ for $x \in \partial\Omega$, which means that the sets $\Omega\backslash\Omega_h$ and $\Omega_h\backslash\Omega$ are embedded in sets of width $Ch|\log h|$ around $\partial\Omega$, thereafter the symmetric difference $\Omega\Delta\Omega_h$ satisfies

$$\Omega\Delta\Omega_h \subseteq \{x \in \Omega : \quad d(x,\partial\Omega) \leq Ch|\log h|\}$$

hence

$$d(\Omega,\Omega_h) \leq Ch|\log h|$$

□

Theorem 3. Let $(\Omega_h, u_{1,h}, u_{2,h})_h$ a sequence of discrete solution's of (26), then the accumulation tuple (Ω, u_1, u_2) solves (9).

Proof. Consider $(\Omega_h, u_{1,h}, u_{2,h})_h$ a solution sequence of the discrete optimal problem (26), let (Ω, u_1, u_2) denote the accumulation points of the sequence $(\Omega_h, u_{1,h}, u_{2,h})_h$, we have to prove that the tuple (Ω, u_1, u_2) solves (9). By theorem 2 implies that $u_{1,h}$ and $u_{2,h}$ converge to u_1 and u_2 as $h \to 0$ respectively, in addition we have $\lim_{h\to 0} d(\Omega,\Omega_h) = 0$. Note that Ω belongs to Θ_{ad}, also it is easy to show that (u_1, u_2) lives in $\mathrm{U}_1 \times \mathrm{U}_2$, then we have the following convergences

$$\begin{cases} \lim_{h\to 0} \mathcal{E}_1(\Omega_h, u_{1,h}) = \mathcal{E}_1(\Omega, u_1) \\ \lim_{h\to 0} \mathcal{E}_2(\Omega_h, u_{2,h}) = \mathcal{E}_2(\Omega, u_2) \\ \mathcal{J}(\Omega, u_1, u_2) \leq \liminf_{h\to 0} \mathcal{J}(\Omega_h, u_{1,h}, u_{2,h}) \end{cases}$$

To end up this proof we need to ensure that $(u_1, u_2) \in \mathcal{U}_1 \times \mathcal{U}_2$, we already have that u_1 and u_2 satisfy the weak formulation (3) and (5), it remains to show that $u_1 = g_1^\rho$ on Γ_1 and $\int_{\partial\Omega} u_2 ds = 0$, which can be obtained using the above convergences, thus (Ω, u_1, u_2) is an optimal solution of (9).

□

5 | ADAPTIVE MESH REFINEMENT

As we have mentioned in the introduction, if a domain has some corners then the approximation with FEM may not achieve its high performance, therefore the need to create and adapt a new triangulation with smaller triangles in the neighborhood of each

corner. Before that, a posteriori error estimate must be established, it will help to refine a given triangulation with the refinement indicator.

Definition 3. Consider $u_h \in C^1\left(\mathcal{T}_h\right)$ and $E \in \mathbb{E}_h$ an interior edge, in other word there exist two distinct triangles T_1 and T_2 such that $E = T_1 \cap T_2$. we introduce the jump of ∇u_h in normal direction across E by the following

$$\left[\nabla u_{i,h} \cdot \nu_E\right] = \nabla u_{i,h}\big|_{T_1} \cdot \nu_{T_1,E} + \nabla u_{i,h}\big|_{T_2} \cdot \nu_{T_2,E} \quad \text{for} \quad i = 1, 2,$$

with $\nu_{T_1,E}$ and $\nu_{T_2,E}$ are the normal outer unit vectors on E to T_1 and T_2 respectively.

Let define for $i = 1,\ 2$

$$\mathbb{E}_{i,D} = \left\{E \in \mathbb{E}_h,\ E \subseteq \Sigma_i\right\} \quad \text{and} \quad \mathbb{E}_{i,N} = \left\{E \in \mathbb{E}_h,\ E \subseteq \Sigma_{3-i}\right\}.$$

Remark 2. For $i = 1, 2$, if $E \in \mathbb{E}_{i,D}$ then $\left[\nabla u_{i,h} \cdot \nu_E\right] = 0$.

Let consider now the residual function R defined by[14], for $i = 1, 2$

$$R_E(u_{i,h}) = \begin{cases} -\left[\nabla u_{i,h} \cdot \nu_S\right] & \text{if } E \in \mathbb{E}_h, \\ g_{2,h} - A\nabla u_{i,h} & \text{if } E \in \mathbb{E}_{i,N} \end{cases}$$

Definition 4. For $i = 1, 2$, we define the refinement indicator $\eta_{i,T}$ by the following, for all $T \in \mathcal{T}_h$

$$\eta_{i,T}^2 = h_T^2 \|f_h + \Delta u_{i,h}\|_{0,T}^2 + \sum_{E \in \mathbb{E}_h,\ E \subset \partial T} h_E \left\|R_E(u_{i,h})\right\|_{0,E}^2. \tag{30}$$

Now we announce the a posteriori error estimate result[13,14].

Proposition 1. There exist two constants c_5 and c_6 such that, for $i = 1, 2$ we have the estimate

$$\left|u_i - u_{i,h}\right|_{1,\Omega} \leqslant c_5 \left[\sum_{T \in \mathcal{S}_h} \left(\eta_{i,T}^2 + h_T^2 \left\|f - f_h\right\|_{0,T}^2\right) + \sum_{E \in \mathbb{E}_{i,N}} h_E \left\|g_2 - g_{2,h}\right\|_{0,E}^2\right]^{\frac{1}{2}}$$

with h_T and h_E are the diameter and the length of T and E respectively.

We have also for all T in $\mathcal{T}_h$

$$\eta_{i,T} \leqslant c_6 \left[\left|u - u_{1,h}\right|_{1,\omega_T}^2 + \sum_{T' \subset \omega_T} h_{T'}^2 \left\|f - f_h\right\|_{0,T'}^2 + \sum_{E \in \mathbb{E}_{i,N}} h_E \left\|g_2 - g_{2,h}\right\|_{0,E}^2\right]^{\frac{1}{2}}$$

with $w_T = \bigcup_{\mathbb{E}(T) \cap \mathbb{E}(T')} T'$. The constant c_5 and c_6 are from[14].

The proof of this proposition is quite similar to the results in[14]. In algorithm 1 we describe the general steps to perform a mesh refinement.

Algorithm 1. Consider a mesh size h, $\alpha \in]0, 1[$, $\varepsilon_1 > 0$ and set $k = 0$

1. Initialize the triangulation $\mathcal{T}_k$
2. **For** i=1,2
3. Compute the state solutions $u_{i,k}$
4. For every $T \in \mathcal{T}_k$ compute $\eta_{i,T}$ using (30)
5. Stop if $\eta_{i,T} \leq \varepsilon_{\text{stop}}$
6. Choose the set of marked elements $\mathcal{M}_k \subset \mathcal{T}_k$ according to $\sum_{T \in \mathcal{M}_k} \eta_{i,T} \geq \alpha \sum_{T \in \mathcal{T}_k} \eta_{i,T}$
7. Refine every element $T \in \mathcal{M}_k$, then create the new triangulation $\mathcal{T}_{k+1}$
8. **End**
9. Set $k = k + 1$ and back to step (2).

The parameter α controls the refinement, in other word the smaller α the finest mesh we can obtain.

There is several choices to refine a marked element, we cite for example the Red-Green-Blue (RGB) refinement and the edge bisection refinement [15,16]. In this work we chose the RGB refinement technique.

Definition 5. The RGB refinement is defined as a performance of the following steps

1. Red-refinement consists in dividing a element into four sub-elements by attaching the midpoints of its edges.
2. Green-refinement attend to divide an element into two sub-elements by joining the longest edge's midpoint with the vertex of its opposite.
3. Blue-refinement consists in dividing an element into three sub-elements. First we perform the green-refinement, then we join the midpoint of one of the unrefined edges with the new vertex.

Now we supply algorithm 1 with new sub-steps at the step number 7.

Algorithm 2. Consider $\mathcal{M}_h^k \subset \mathcal{T}_h^h$ the set of elements marked.

1. Mark all edges $E \in \mathbb{E}_h^k$ in a triangle T from $\mathcal{M}_h^k$
2. Mark all the longest edges in $\mathcal{T}_h^k$.
3. Refine the marked element according to the RGB refinement.

6 | DESCRIPTION OF THE PROPOSED SCHEME

In this section we will introduce the iterative scheme to solve the optimal control problem (9). The first part concern the description of the steps of the conjugate gradient method. The second part is dedicated to discuss the initialization of the gradient method.

6.1 | Conjugate gradient with Wolfe conditions

We consider the conjugate gradient method to update iteratively an initial domain $\Omega^0 \in \Theta_{ad}$ by the following scheme

$$\Omega^{n+1} = \Omega^n + \beta^n P^n. \tag{31}$$

with ξ^n is the search step size. The directions of descent P^n are obtained as solution of the linear system:

$$P^n = -d\mathcal{J}^n + \gamma^n P^{n-1} \tag{32}$$

where $d\mathcal{J}^n$ is the shape gradient at iteration n, the conjugate coefficient [17] γ^n is given by

$$\gamma^n = \frac{\langle dJ^{n+1} - dJ^n, dJ^{n+1}\rangle}{\langle dJ^n, dJ^n\rangle}, \tag{33}$$

To compute the search step size we may use the sensitivity calculus which will involve the sensitivity problem [18,4], otherwise we can use some line search methods, such as the backtracking or the Armijo line search methods [19,20]. In this application we will use the Armijo line search technique, it requires that β^n must meet the sufficient decrease and the curvature conditions. The first condition is satisfied with the following inequality,

$$\mathcal{J}(\Omega^n + \beta^n P^n) \leq \mathcal{J}(\Omega^n) + \delta_1 \beta^n \langle d\mathcal{J}^n, P^n\rangle \tag{34}$$

with $\delta_1 \in [0, 1]$, usually we chose the coefficient ρ_1 to be fairly small, we set $\delta_1 = 10^{-4}$.

The second condition, will ensure that the sufficient decrease condition will not stuck in short steps, it guarantee the decrease of $\mathcal{J}$ follows a reasonable progress. This curvature condition reads, for some $\delta_2 \in [\delta_1, 1]$

$$\langle dJ(\Omega^n + \beta^n P^n), P^n\rangle \geq \delta_2 \beta^n \langle dJ^n, P^n\rangle \tag{35}$$

We refer to [19] for the existence proof of step sizes that meet the Wolfe conditions.

6.2 | Initialization with genetic algorithm

The convergence of gradient methods always depends on the choice of the initial guess, first it must belong to the admissible shape set, then it must be well chosen. It is harder to pick it manually, thus an heuristic method may do the work.

Genetic algorithms[21,22] (GAs) are one of the most famous heuristic methods. They seek to find the best optimal solution in a population of possible solutions. Starting with a random population of candidate solutions called individuals, GAs move to a new population using the genetic operations. The first stage is the selection operation, it helps to choose the parents for the future generation based on the fitness of individuals. In this work we consider the tournament selection operation. The crossover operation aims to generate a new offspring using two parents, in our work we chose the random barycentric crossover. The last operation is the mutation, it consist to add some diversity in the new generation, for our algorithm we use the non-uniform mutation operator.

The time complexity of genetic algorithms depends on the number of generations, the population and individual sizes. To have smooth free boundaries we have to discretize with a large number, then the size of individuals becomes larger, which augment the time complexity. To overcome this issue and reduce the size individuals, we use the Bézier curve[23] to parameterize the free boundaries. That means we will only give few control points to draw the free boundaries. Some advantages of Bézier curves is that they produce a continuous, differentiable curve.

Now we write all the steps of the proposed scheme in algorithm 3.

Algorithm 3. Choose ε_2, ε_2, N_{max1}, N_{max2}, $P^0 = 0$, $\gamma^0 = 0$, set $n = 0$.

1. Generate an initial population
2. **While** $n < N_{max1}$
3. Solve the state problems (3) and (5) for each individual.
4. Apply the selection, then extract the best individual Ω_{best}.
5. Stop if $\mathcal{J}(\Omega^n_{best}, u^n_1, u^n_2) < \varepsilon_2$.
6. Perform the genetic operator crossover then the mutation operation to create the new generation.
7. Set $n = n + 1$ and back to step 3.
8. **end**
9. set $\Omega^0 = \Omega_{best}$ and $n = 1$.
10. **While** $n < N_{max2}$
11. Find an adaptive mesh for Ω^n using algorithm 1.
12. Compute u^n_1 and u^n_2 solutions of (3) and (5).
13. Stop if $\mathcal{J}(\Omega^n, u^n_1, u^n_2) < \varepsilon_3$.
14. Find λ^n_i solutions of adjoint problems for $i = 1, 2$.
15. Compute the shape gradient $d\mathcal{J}^n$ using (16)
16. Manipulating (33) update the conjugate coefficient γ^n.
17. Update the direction $P^n = -d\mathcal{J}^n + \gamma^n P^{n-1}$.
18. Find β^n satisfying the Armijo conditions (34) and (35).
19. perform the update $\Omega^{n+1} = \Omega_n + \beta^n P^n$.
20. Set $n = n + 1$, and back to step 11.
21. **end**

7 | NUMERICAL RESULTS AND DISCUSSION

In this section, we perform some numerical test in order to show the validity of the theoretical results. First we assume that the state problems (2) and (4) have the exact solution:

$$u(x, y) = exp(x + y), \qquad x, y \in \Omega(\varphi, \psi)$$

For the sake of simplicity we consider that $A(x) = 1$, the rest of the functions f, g_1 and g_2 are constructed from the above exact solution. The discretization of each admissible domain is a uniform grid of size $N \times M$, we take $N = 8$ and $M = 16$, at each mesh regeneration, we apply algorithm 1. In figure 2 we illustrate the adaptively refined mesh for one of the examples below.

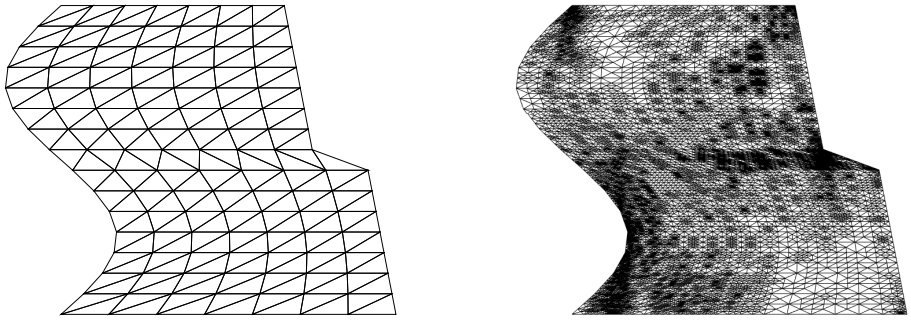

FIGURE 2 Example of an adaptively refined mesh.

As we said before, the initial guess for the conjugate gradient method is generated with the genetic algorithm, for that we consider the setting of the GA algorithm in the next table The maximum generations number is the same N_{max1} number in

TABLE 1 GA parameters

Population size	Max generations	Crossover ration	mutation ratio
25	5	75%	5%

algorithm 3, the rest of the parameters in algorithm 3 are given as follows, $N_{max2} = 100$, the tolerance $\varepsilon_1 = 1e - 1$ and $\varepsilon_2 = \varepsilon_3 = 1e - 5$. The control parameter α in the mesh refinement algorithm is set to 0.05. The coefficients δ_1 and δ_2 in the Armijo conditions are set to $1e - 4$ and 0.9 respectively. For the choice of the regularization parameters[24] we consider that $\varrho_1 = \varrho_2 = 0.01\sqrt{h_l}$ with $h_l = \dfrac{\sqrt{8}}{N}$. The control shape $\mathcal{O}$ is considered as the largest parallelogram included in the exact shape Ω see figure 3 .

We measure the average relative errors between exact $\left(\Gamma_1(\varphi^e), \Gamma_2(\psi^e)\right)$ and obtained optimal boundaries $\left(\Gamma_1(\varphi), \Gamma_2(\psi)\right)$, it is defined by

$$err = \max\left\{\left|\frac{\varphi(y) - \varphi^e(y)}{\varphi^e(y)}\right|, \left|\frac{\psi(y) - \psi^e(y)}{\psi^e(y)}\right|\right\} \tag{36}$$

We shall also show the importance of using the genetic algorithm to estimate the initial guess for the gradient method. In other word, we shall compare minimization using only the conjugate gradient (CG), versus the combined genetic algorithm with the conjugate gradient (GACG). For that, we keep the same steps of the gradient method from step 9 to the end in algorithm 3, then we consider the initial boundaries

$$\Gamma_1^{initial} = \left\{\Big(-1, y\Big) / \ \ y \in [0, 1]\right\} \quad \text{and} \quad \Gamma_2^{initial} = \left\{\Big(3, y\Big) / \ y \in [0, 1]\right\}.$$

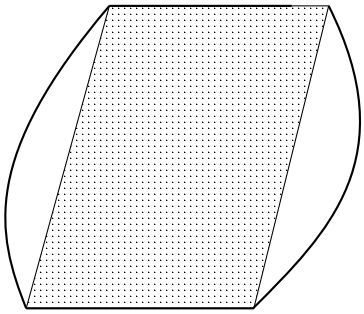

FIGURE 3 The control shape is the dashed region.

Example 1: we seek to identify the exact boundaries Γ_1 and Γ_2:

$$\Gamma_1 = \left\{ \Big(1 - y, y\Big) / \;\; y \in [0,1] \right\} \quad \text{and} \quad \Gamma_2 = \left\{ \Big(2 + y^2, y\Big) / \; y \in [0,1] \right\},$$

The obtained results for this example are illustrated in figure 4 and 5 . It is seen that the genetic algorithm did generate the best initial guess (figure 4). The optimal boundaries matched the exact ones. The cost decay is illustrated the right picture of figure 5 , the proposed algorithm reached the precision 0.01776.

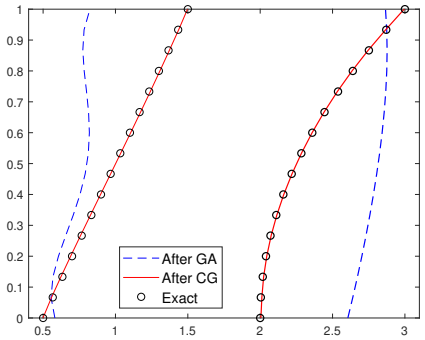

FIGURE 4 The optimal boundaries without noisy data for example 1.

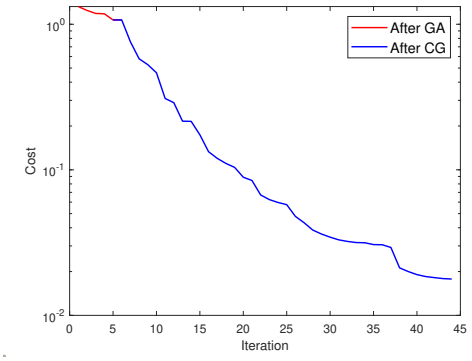

FIGURE 5 The cost decay for example 1.

In figures 6 and 7 we illustrate the comparison of the approximation with GACG and CG algorithms. It is obvious the importance of starting with the genetic algorithm to find an initial guess, the GACG algorithm converge faster then CG algorithm. Moreover, the optimal boundaries of GACG are more accurate.

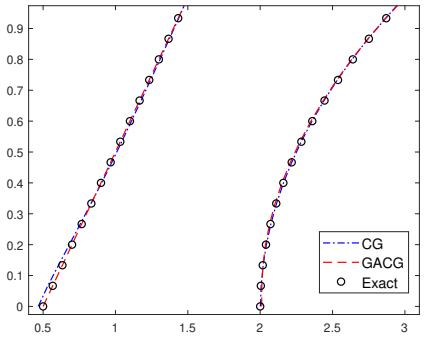

FIGURE 6 Comparison of the optimal boundaries with CG and GACG for example 1

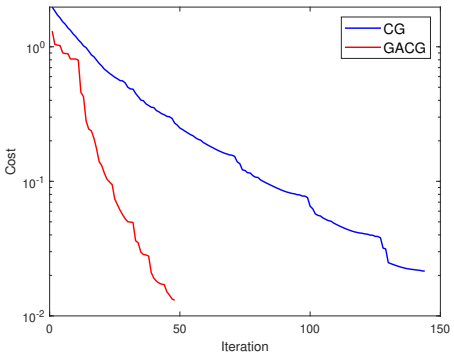

FIGURE 7 Cost decay comparison of the CG and GACG for example 1

Example 2: now we assume that the free boundaries are given by the exact:

$$\Gamma_1 = \left\{ \left(\frac{1}{2} sin(2\pi y), y \right) / \ y \in [0,1] \right\} \quad \text{and} \quad \Gamma_2 = \left\{ \left(3 - \frac{y}{2}, y \right) / \ y \in [0, 0.5] \right\} \cup \left\{ \left(2.5 - \frac{y}{2}, y \right) / \ y \in]0.5, 1] \right\}.$$

The particularity of this example is that Γ_2 has two singularities at the vicinity of 0.5. Although, the obtained numerical results for this example are of good quality, we have plotted in figure 8 the optimal boundaries versus the exact ones and the cost decay with respect to the iteration number.

Again we show the comparison of the GACG and CG algorithms, it is seen the huge difference between the obtained results, the CG does not converge for this example with the above initial guess, in contrast the GACG did.

We try again with the CG algorithm with new initial boundaries

$$\Gamma_1^{initial} = \left\{ \left(1, y \right) / \ \ y \in [0,1] \right\} \quad \text{and} \quad \Gamma_2^{initial} = \left\{ \left(4, y \right) / \ y \in [0,1] \right\}.$$

The new obtained results for the CG algorithm were of good quality as figures 11 and 12 show, both optimal boundaries matched the exact ones, we only remark that the CG algorithm takes more iterations to converge. We conclude that to ensure the convergence of gradient method we make sure to chose the right initial guess, which is harder to do manually, thus the importance of using genetic algorithms to find the best initial guess. At this end, the obtained numerical results proves the efficiency of the proposed scheme.

With noisy data: Before testing the proposed algorithm for the case with noisy the data, we first shall construct the noisy measurement g_1^ρ and g_2^ρ of the exact data g_1 and g_2, for that we set $g_1^\rho = g_1 + \rho R_1$ and $g_2^\rho = g_2 + \rho R_2$, with R_1 and R_2 are two random vector uniformly distributed in $[0, 1]$, ρ is the noise level. Now we can turn our proposed algorithm to identify the exact boundaries in the two last examples for different level of noise. We write in table 2 the achieved cost and the total number of iterations (Iter), for different noise level. In figure 13 and 14 we illustrate the obtained optimal boundaries.

It is seen that the quality of the optimal boundaries decrease with respect to the noise level. As the noise level increases we remark that the cost and the relative error increases, and the number of iteration as well, especially in example two, which is

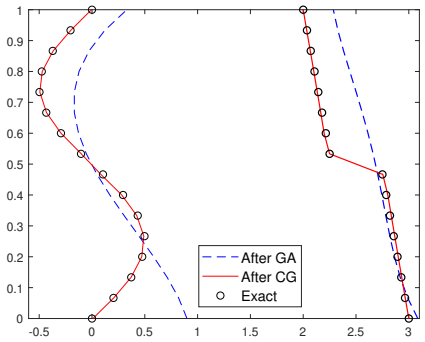

FIGURE 8 The optimal boundaries without noisy data for example 2.

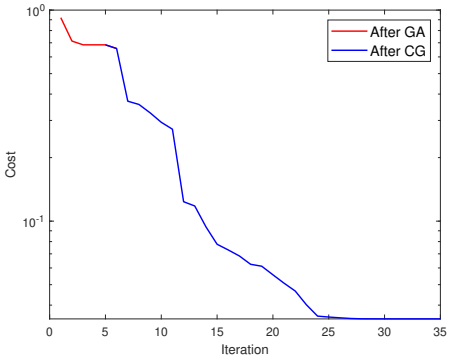

FIGURE 9 The cost decay for example 2.

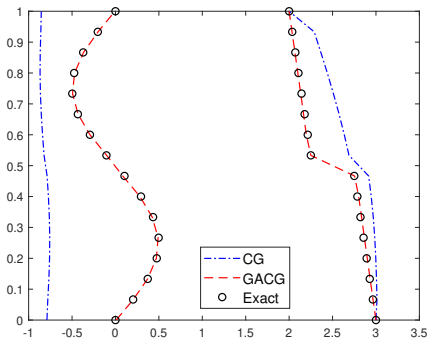

FIGURE 10 Comparison of results obtained with CG and GACG for example 2.

normal due to the complexity of the configuration of the exact boundaries. However the obtained boundaries remain a good approximation of the exact boundaries.

8 | CONCLUSION

In this paper we have proposed a class of bilateral free boundaries problem. After establishing the optimal control problem, we have proved its optimal solution existence's. The first optimality conditions and the shape gradient are computed. The iterative method used in this paper, is based on genetic algorithm guided conjugate gradient combined with the finite element method. To improve the approximation with FEM, we used a mesh refinement at each mesh regeneration. We illustrated different numerical

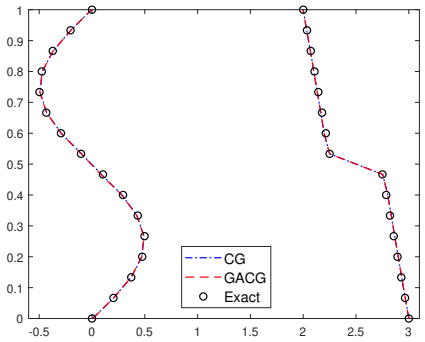

FIGURE 11 Comparison of optimal boundaries with CG and GACG for example 2 with the new initial guess.

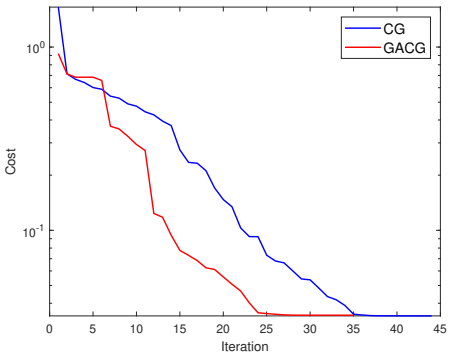

FIGURE 12 Cost decay comparison of CG and GACG for example 2 with the new initial guess.

TABLE 2 The optimal cost with noisy data

Noise level	Example 1			Example 2		
	Cost	err	Iter	Cost	err	Iter
0%	0.01776	0.00284	48	0.03442	0.00485	36
1%	0.02607	0.00689	50	0.08383	0.01981	38
5%	0.06848	0.02847	51	0.10230	0.03102	43
10%	0.10035	0.03441	55	0.16009	0.04998	70

examples to demonstrate the efficiency of the proposed iterative scheme. In all numerical experiences, the identification of the bilateral free boundaries works very well in both cases, with and without noisy measurement. We have remarked that, the quality of the approximation deceases while the noise level increases, even thought the numerical results still acceptable. At this end, the proposed scheme is efficient and robust to solve similar kind of inverse identification problems.

References

1. Barboteu M., Bartosz K., Kalita P. An analytical and numerical approach to a bilateral contact problem with nonmonotone friction. *International Journal of Applied Mathematics and Computer Science.* 2013;23(2):263–276.

2. Huang C. H., Shih C. C. A shape identification problem in estimating simultaneously two interfacial configurations in a multiple region domain. *Applied Thermal Engineering.* 2006;26(1):77–88.

3. Mozaffari M. H., Khodadad M., Dashti-Ardakani M. Simultaneous identification of multi-irregular interfacial boundary configurations in non-homogeneous body using surface displacement measurements. *Journal of Mechanical Engineering*

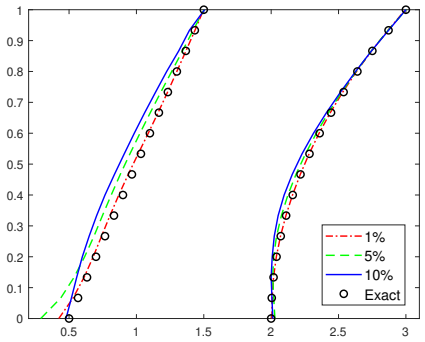

FIGURE 13 The optimal boundaries with noisy data for example 1.

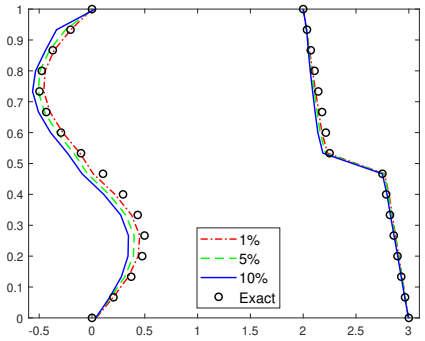

FIGURE 14 The optimal boundaries with noisy data for example 2.

Science. 2016;231(13):1–12.

4. Zolesio J. P., Sokolowski J. *Introduction to Shape Optimization Shape Sensitivity Analysis*. Springer, Berlin, Heidelberg; 1992.

5. Bergounioux M., Lenhart S. Optimal Control of Bilateral Obstacle Problems. *SIAM Journal on Control and Optimization.* 2004;43(1):240–255.

6. Hinze M., Ziegenbalg S. Optimal control of the free boundary in a two-phase Stefan problem. *Journal of Computational Physics.* 2007;223(2):657–684.

7. Dashti-Ardakani M., Khodadad M. Shape estimation of a cavity by inverse application of the 2D elastostatics problem. *International Journal of Computational Methods.* 2013;10(06):1350042.

8. El Yazidi Y., Ellabib A. Reconstruction of the depletion layer in MOSFET by genetic algorithms. *Mathematical Modeling and Computing*. 2020;7(1):96–103.

9. Banichuk N. V., Barthold F. J., Falk A., Stein E. Mesh refinement for shape optimization. *Structural optimization.* 1995;9(1):46–51.

10. Kohno H., Tanahashi T. Numerical analysis of moving interfaces using a level set method coupled with adaptive mesh refinement. *International Journal for Numerical Methods in Fluids.* 2004;45(9):921–944.

11. Cea J. Conception optimale ou identification de formes, calcul rapide de la dérivée directionnelle de la fonction coût. *Modélisation mathématique et analyse numérique.* 1986;20(3):371–402.

12. Ciarlet P. G. Basic error estimates for elliptic problems. In: Handbook of Numerical Analysis, vol. 2: Elsevier 1991 (pp. 17–351).

13. Bartles S. *Numerical Approximation of Partial Differential Equations*. Springer; 2016.

14. Verfürth R. A posteriori error estimation and adaptive mesh-refinement techniques. *Journal of Computational and Applied Mathematics.* 1994;50(1):67–83.

15. Chen L., Zhang C. A coarsening algorithm on adaptive grids by Newest Vertex Bisection and its applications. *Journal of Computational Mathematics.* 2010;28(6):767–789.

16. Funken S. A., Schmidt A. Adaptive Mesh Refinement in 2D – An Efficient Implementation in Matlab. *Computational Methods in Applied Mathematics.* 2019;(0).

17. Luenberger D. G., Ye Y. *Linear and Nonlinear Programming*. Springer US; 3 ed.2008.

18. Haslinger J., Mäkinen R. A. E. *Introduction to shape optimization: theory, approximation, and computation*. SIAM; 2003.

19. Nocedal J., Wright S. J. *Numerical Optimization*. Springer, New York, NY; 2006.

20. Lewis R. M., Torczon V., Trosset M. W. Direct search methods: then and now. *Journal of Computational and Applied Mathematics.* 2000;124(1):191–207.

21. Holland J. H. *Adaptation in Natural and Artificial Systems: An Introductory Analysis with Applications to Biology, Control, and Artificial Intelligence*. MIT Press; 1992.

22. McCall J. Genetic algorithms for modelling and optimisation. *Journal of Computational and Applied Mathematics.* 2005;184(1):205–222.

23. Prautzsch H., Boehm W., Paluszny M. *Bézier and B-Spline Techniques*. Springer, Berlin, Heidelberg; 2002.

24. Hanke M., Engl H. W., Neubauer A. *Regularization of Inverse Problems*. Springer, Mathematics and Its Applications; 2000.